ELSEVIER

Variable optical attenuator using a thermal actuator array with dual shutters

J.C. Chiou [*], W.T. Lin

Department of Electrical and Control Engineering, National Chiao Tung University, 1001 Ta Hsueh Road, HsinChu 30010, Taiwan

Abstract

A compact variable optical attenuator (VOA) driving by thermal actuating principle with dual shutters for single mode fibers is developed. The fabricated thermal actuator array is capable of achieving larger displacement with low applied voltage than traditional thermal actuator array. The designed dual shutters can be driven independently or simultaneously, which increase the accurate tuning range and decrease working voltage for variable optical attenuator. The device is fabricated using MEMS-SOI fabrication technology, which greatly simplifies the traditional surface micromachining technology and increases its corresponding reliability. The newly designed thermal actuator array is capable of traveling 20 μm distance with less than 5 V applied voltage for VOA application. The insertion loss of the fabricated VOA is below 1.5 dB. The initial return loss and working return loss is about 50 and 40 dB, respectively. Experimental results indicated that the response time is below 4 ms and maximum attenuation range is about 40 and 45 dB at 1550 and 1310 nm, respectively. The working voltage and temperature of the designed VOA is under 5 V and 550 K, respectively.

1. Introduction

Variable optical attenuators (VOA) with large attenuation range and high response time play an increasingly important role in fiber-optic networks. The main applications of VOA are in power tuning of lasers and detectors, in gain control and flattening of optical amplifiers and in optical device protection. Note that when optical signals traveling in fibers for several kilometers their intensity will become weakened due to the variations in source powers, absorption and scattering in transmission, and bending losses in the fiber network. Typically, when signal intensity falls under a certain threshold, erbium-doped fiber amplifier (EDFA) is used to amplify the signal. In WDM, VOA plays an important role in equalizing different channel's intensity before signals are amplified by EDFA.

Commercially available variable optical attenuators are mainly based on optomechanical principles. They have the characteristics of low insertion loss (<1.5 dB), low cross-talk, wavelength

[*] Corresponding author. Tel.: +886-3-5731881; fax: +886-3-5715998.

E-mail address: chiou@cc.nctu.edu.tw (J.C. Chiou).

uniformity, large attenuation range (>50 dB), low wavelength dependent loss (WDL), and low polarization dependent loss (PDL). However, the drawbacks of the existing VOAs are large in size, low operating speed, high cost and uncertain reliability. Due to the advanced MEMS fabrication technologies, MEMS optical devices can overcome the above-mentioned problems by integrating fabricated chips with single mode fiber.

Different types of MEMS VOAs have been developed previously [1–13]. We characterized the VOAs by its attenuation principles and driving methods. According to attenuation principles, wave guide-based VOAs can achieve high-speed response time easily. However it has difficulty to reach a large attenuation range with low insertion loss [1,2]. VOAs based on an optical shutter or reflective mirror can achieve large attenuation range. However optical shutter types have a problem of higher PDL and it can be improved by modifying the shutter shape [8,10]. One of reflective mirror types has poor WDL, which generally use bulk optics and needs an additional mount to fix optical fibers [3–6].

Optical shutter types or reflective mirror types VOAs that are driven by electrostatic force are able to achieve large displacement with high driving voltage or numerous comb-fingers [6–10]. The more comb-fingers the larger displacement can be obtained and in return we increase the actuator mass and decrease response time. Existing thermal type VOA device uses the thermal arch beam approach, which is capable of achieving large displacement with low driving voltage [11,12]. Unfortunately, its fabrication method is complicated in realization. Nevertheless, it proves that single crystal silicon has advantage of being simple to heat and providing inherent ambient temperature compensation.

In order to overcome the above mentioned drawbacks in thermal type VOA. A variable optical attenuator using the newly developed thermal actuator array with dual shutters is developed. The thermal actuator array can achieve larger displacement (>20 μm) with low voltage (<5 V) than traditional thermal actuator array. Note that the designed dual shutters can be driven independently or simultaneously, which increase the tuning range

for variable optical attenuator and decrease working voltage. The device is fabricated using MEMS-SOI fabrication technology, which simplifies the traditional surface micromachining technology. Moreover, by using single crystal silicon as thermal actuator array material increases its reliability as mentioned previously by Wood et al. Furthermore, in order to improve the assembly efficiency, 80 μm depth fibers alignment grooves are fabricated at the same substrate along with the thermal actuator array.

2. The configuration of proposed variable optical attenuator

2.1. Device structural design

In the present study, the attenuator chip is designed to ease the fiber assembly process. Here, fiber alignment grooves with the size of 126 μm width and 80 μm depth are fabricated on the same SOI device wafer to increase final alignment efficiency. Moreover, dual shutters and fiber-end stopper are fabricated sufficiently small in order to bring fiber ends closer together. The two fibers are arranged horizontally and separated approximately 20 μm in distance. According to theoretical calculation, the longitudinal offset effect produces the beam divergence loss. Here, the loss can be calculated using the following equations:

$$Z_R = \pi n W_G^2 / \lambda, \tag{1}$$

$$\eta = \frac{1}{1 + (0.5^* Z_w / Z_R)^2}, \tag{2}$$

where Rayleigh distance (Z_R) denotes the beam wave that is radiated from the fiber end into a homogeneous medium; n is the refractive index; W_G is the core diameter (5 μm); and λ denotes the wavelength (1.55 μm); by using Eq. (1), the Rayleigh distance Z_R is equal to 50.6708 μm. Since the longitudinal offset distance, Z_w is equals to 20 μm, from Eq. (2), the theoretical light loss due to the beam divergence is about 0.16 dB ($\log_{10} \eta$).

The advantages of using dual shutters are: (1) decrease applied driving voltage; (2) produce nearly linear response in voltage vs. attenuation by altering

the total voltage (voltage sum between two thermal actuator arrays) vs. total displacement function [14]. In order to avoid back-reflection from the input light on the shutter and output fiber back into input fiber, the shutter as well as the fiber end face is aligned at an 82° angle with respect to fiber alignment groove and fiber end face is 8° angle polished with antireflective coating. In order to improve the poor PDL characteristic of shutter type VOAs, the shutter end face is designed in profiled blade with small angle (as shown in Fig. 6). For the present VOA design, the device is required to possess large overall displacement and low driving voltage in order to produce large attenuation range. To drive the shutters into the optical path of the fiber, a newly developed thermal actuator array is used. The VOA design can be realized using MEMS technology as schematically shown in Fig. 1.

2.2. Actuator design

Simple and effective actuators can be designed and manufactured using thermal effect in silicon [15,16]. It is known that thermal actuators can produce larger displacement than electrostatic force with low applied voltages. A typical U-shaped lateral electro-thermal actuator generates deflections through asymmetric heating of the narrower hot and wider cold beams. The higher current density in the narrower hot beam causes it to heat and expand more than the cold beams. The beams are joined at the free end which forces the actuator tip to move laterally. According to the principle, a horizontal pair thermal actuator combines tethers with a shutter that cancels out their arcing and expanding motion, producing a purely linear motion of the shutter.

The shape of tethers plays an important role in determining the motion efficiency of thermal actuator array. One of the presented thermal actuator array with 80 μm thickness comprise single crystal silicon is illustrated in Fig. 2. The main differences of the designed actuator arrays are in the tether shape, tether size and the connection location with actuators. In the present simulation, the dimensions of different type actuator array are shown in Table 1. The design is simulated by commercial software, CoventorWare. In order to
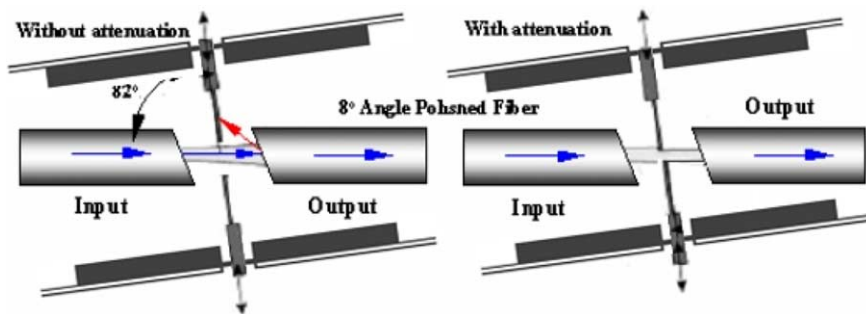

Fig. 1. Schematic of proposed optical variable attenuator with two-way shutters.
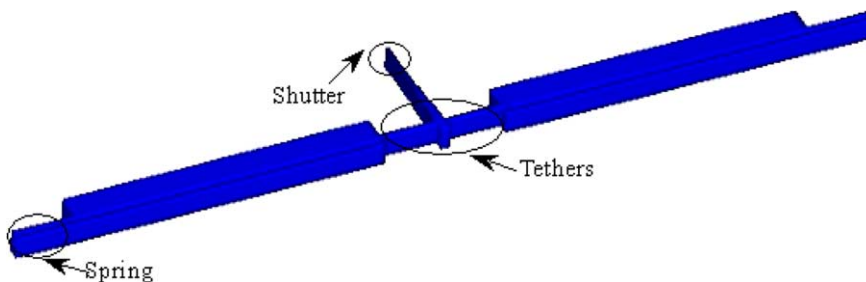

Fig. 2. The schematic drawing of cross-type thermal actuator.

Table 1
The dimensions of five different VOA designs

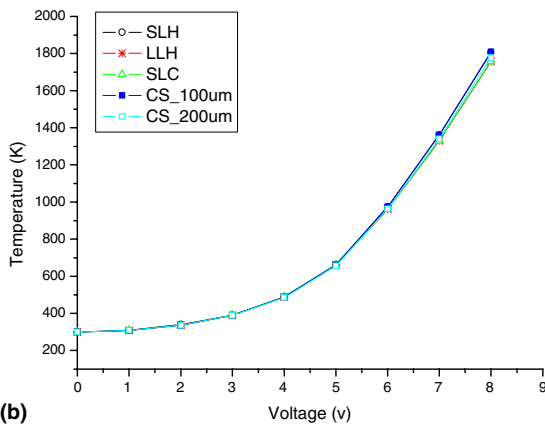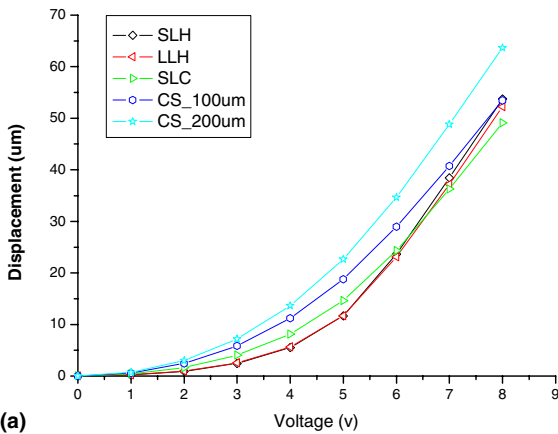| Actuator name	SLH (μm)	LLH (μm)	SLC (μm)	CS_200 (μm)	CS_100 (μm)
Cold beam width	100	100	100	100	100
Cold beam length	995	995	995	995	995
Hot beam width	10	10	10	10	10
Hot beam length	1195	1195	1195	1195	1095
Spring width	10	10	10	10	10
Spring length	200	200	200	200	100
Tether width	15	15	15	15	15
Tether length	103	183	103	180	180
Tether type					

(a)

(b)

Fig. 3. (a–b) The simulation data of deflection and highest temperature vs. applied voltage for different thermal actuators.

compare with the different tether designs, the material properties of single crystal silicon are given as follow: Young's modulus $E = 170$ GPa, Poisson ratio $= 0.25$, coefficient of thermal expansion CTE $= 2.5E-6$, resistivity $\rho = 1E-2$ Ω cm. Here, the temperature-dependent parameters such as variation of thermal conductivity and specific heat are extracted from [17].

With these data, the displacement of the thermal actuator array affected by applied voltage can be simulated and the characteristics of the thermal actuator are obtained. The thermal actuator with different tether designs is also under investigation where the relationship of applied voltage vs. displacement and temperature are shown in Fig. 3(a) and (b). By examining the simulation results, we note that the CS-type thermal actuator arrays produce the most efficient displacement than other designs [14]. All of the simulated maximum temperature is similar due to the fact that the resistance ($\sim$180 Ω) is determined by hot beam. According to the simulation results, we concluded that for identical thermal actuator with different connected tether locations and tether shape play the major factors in affecting the displacement of the shutter.

3. Fabrication technology

The advantage of using the silicon-on-insulator (SOI) technology is to greatly simplify the fabrication process of MEMS devices. However, in processing SOI wafer, the most critical step is the inductive coupling plasma (ICP) etching that determines the final outcome of the structure and the surface roughness of sidewall in fabricating designed optical devices.

The fabrication steps of the MEMS based VOA are shown in Fig. 4(a)–(g). Here, the chosen SOI wafer for the fabrication process is a 500 µm thickness substrate, 2 µm thickness buried oxide layer and 80 µm thickness device wafer with 0.01 Ω cm resistivity (Fig. 4(a)). The reason that we choose 80 µm thickness device wafer is to produce sufficient fiber alignment groove depth for future embedded fiber. In the first step of the fabrication process, lift-off technology is used to deposit chromium and gold for the purpose of finishing connecting pads (Fig. 4(b)). This step avoids difficult photolithography process after deep silicon

etching is performed. Secondly, we use the photolithography to pattern the designed thermal actuator and fiber alignment groove (Fig. 4(c)). The photoresist is then used to dry etch the device wafer by ICP (Fig. 4(d)). The buried oxide serves as an etching stop for ICP for the reason that etching rate is affected by the size of etching area. Note that etching rate will vary for different depth that affects the roughness on the sidewall. Once ICP etching is completed, resist is moved by acetone. To release the structures, the buried oxide has to be removed using BOE (Fig. 4(e)). Etching holes are opened to decrease etching time that is depending on undercutting effect. To avoid metal that is deposited on the top of the thermal actuator, which may produce bimorph effect, shadow mask technology is applied. Gold is deposited by
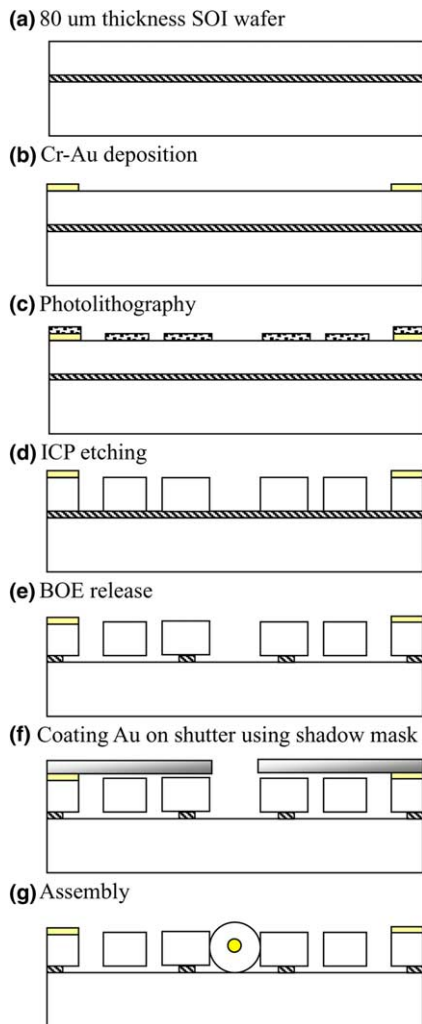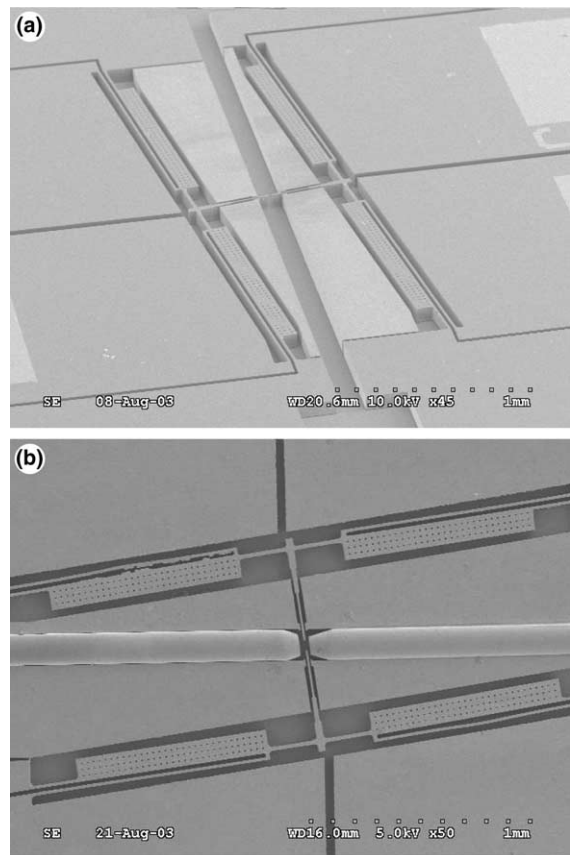

Fig. 4. The fabrication process of the VOA.

Fig. 5. The SEM view of CS_typeattenuator: (a) without optical fibers and (b) with optical fibers.

sputter that increases the reflectivity of shutter (Fig. 4(f)). By integrating optical fiber in alignment grooves with thermal actuator, tether and shutter, we are able to assemble the final variable optical attenuator structure (Fig. 4(g)). Fig. 5(a) and (b) shows the SEM view of CS-type attenuator without/with optical fiber.

4. Experimental results

In order to characterize the designed VOA, a fiber alignment mechanism is used to integrate fibers on the fabricated MEMS chip. The equipment consisted of a 3D adjusting rod and rotation rod to adjust fiber misalignment. First, we insert the input fiber onto the mechanism. Note that, the size of the fiber diameter is 125 μm and the tapered tip angle is 8° [18]. By tuning the 3D adjusting rod, we are able to lead the fiber into the fiber alignment groove. Then, by tuning the rotation rod, the orientation of the fiber end face is adjusted until it is parallel to the shutter. UV-glue is injected into etched caves to fix input fiber. After inserted input fiber on the MEMS chip, same alignment procedure is used to insert output fiber with the help of power meter. Fig. 6(a) and (b) shows the final distance (41.4 μm) between two inserted fibers once the assembly processes were completed. Here, the measured distance between two fibers is more than the designed distance. Theoretical light loss due to the beam divergence at this distance is 0.63 dB. Other obstructing factors included the fiber misalignment and imperfect measurement conditions that produce loss at different wavelengths (1310 and 1550 nm) are due to that fact that we use the 1550 nm single mode fiber to measure 1310 nm light source. This may produce higher loss and dispersion in 1310 nm. The final measured insertion loss is 1.23 and 1.54 dB at 1550 and 1310 nm, respectively. The initial return loss is 50 and 56.8 dB at 1550 and 1310 nm, respectively.

The static characteristic of the five thermal actuator arrays is shown in Fig. 7, which is measured by **WYKO** interferometer. Since the simulation and the measured data have similar tendency, thus, in Fig. 8, the static measured and simulation data of deflection and differential temperature vs.
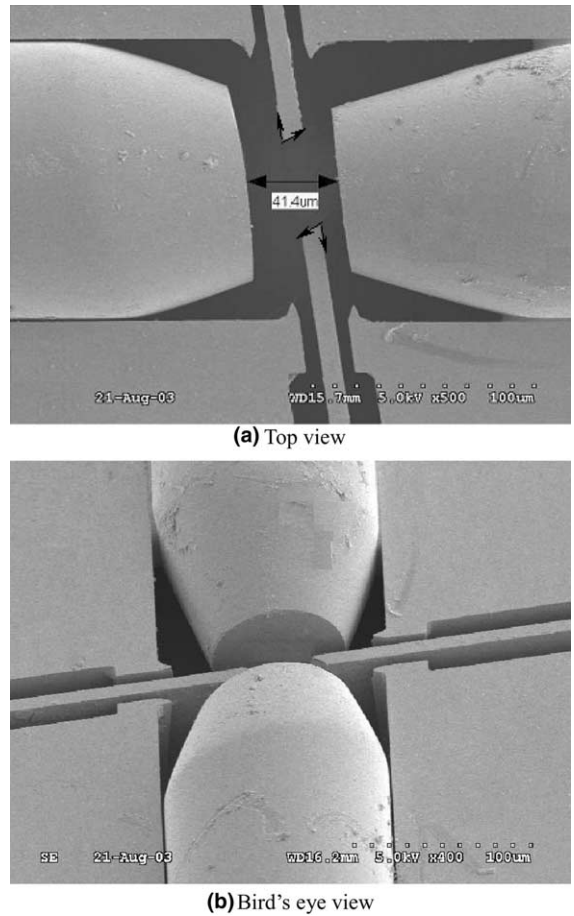

(a) Top view

(b) Bird's eye view

Fig. 6. (a–b) The SEM views of fiber orientation after alignment.
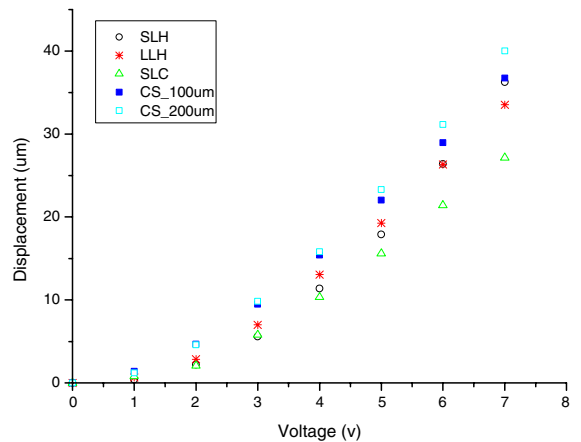

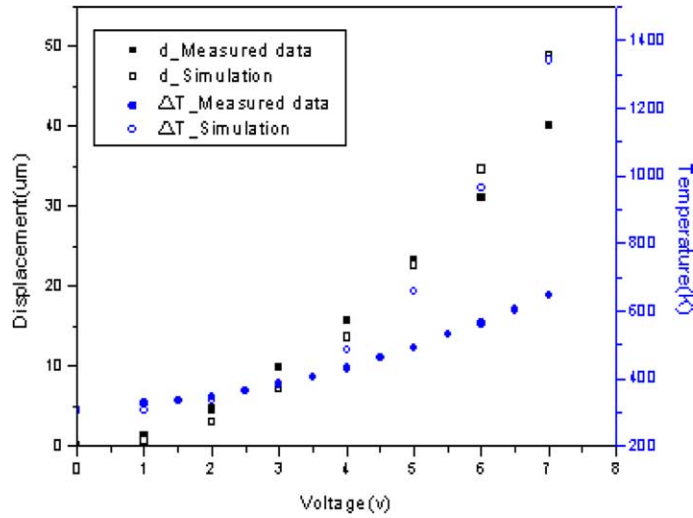Fig. 7. The static measured data of deflections vs. applied voltages.

Fig. 8. The static measured and simulation data of deflection and differential temperatures vs. applied voltages for CS_200_type thermal actuators.
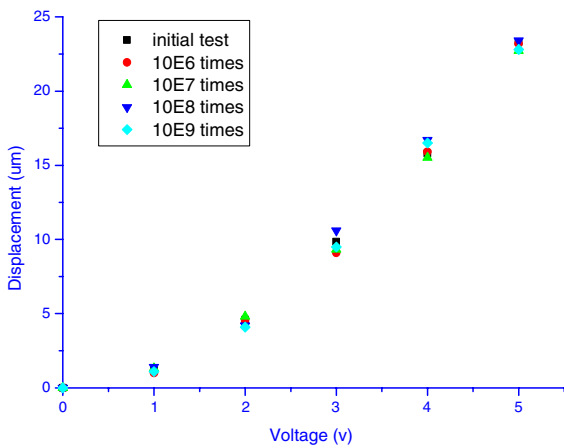

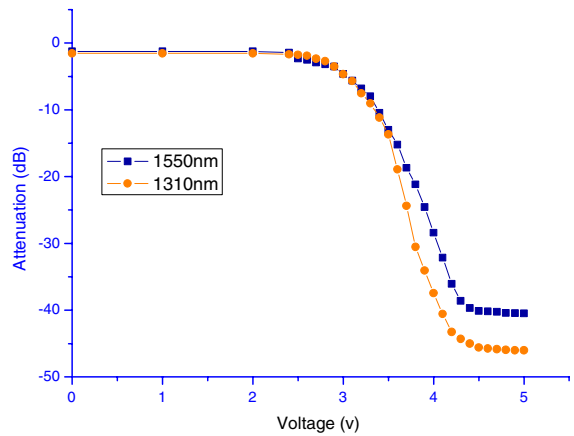Fig. 9. The fatigue test results of the thermal actuator array through 10^9 test cycles.

Fig. 11. The static attenuation vs. voltage characteristics of CS_200_type VOA.

applied voltage for CS-200-typethermal actuators is given. The static temperature data is measured by **QFI** infrared scope. The errors between simu-

lation and experiment are produced by the temperature dependent material properties, gas convection and radiation conductivity that are
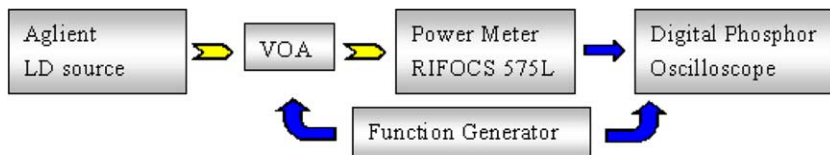

Fig. 10. The schematic measurement structure of VOA.

ignored in the simulations. According to the experiment results, the MEMS based VOA using thermal actuator array design can be driven under 5 V with working temperature under 550 K. Note that, the low working temperature will increase the reliability of the thermal actuator arrays composed of single crystal silicon. Fig. 9 shows the fatigue test results of the thermal actuator array by op-

erating the device 10^9 test cycles. It shows that by using single crystal silicon to manufacture driving component of VOA greatly enhanced the survivability of the device.

When the voltage on the thermal actuator is increased, the shutter is moved into optical path between the input and the output fiber, resulting in attenuation of the coupling. We have tried to im-
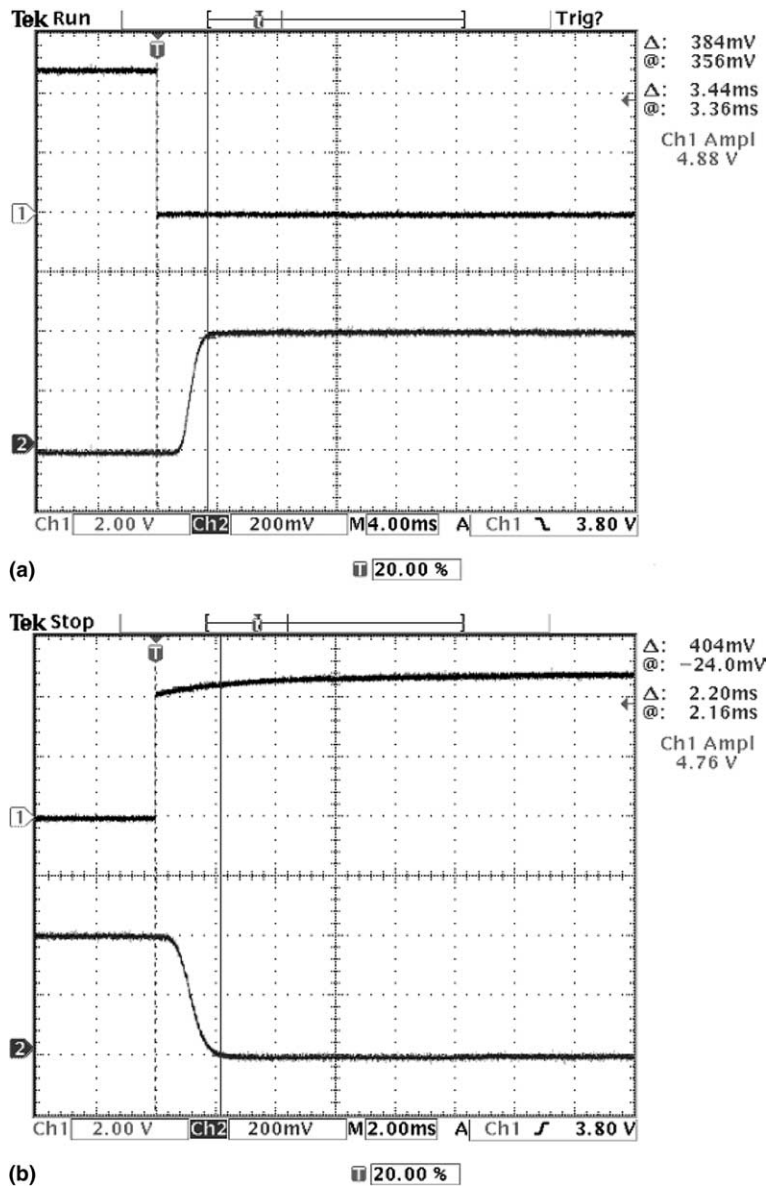

Fig. 12. Dynamic response of CS_200_type VOA: (a) switch OFF → ON: 3.44 ms and (b) switch ON → OFF: 2.20 ms.
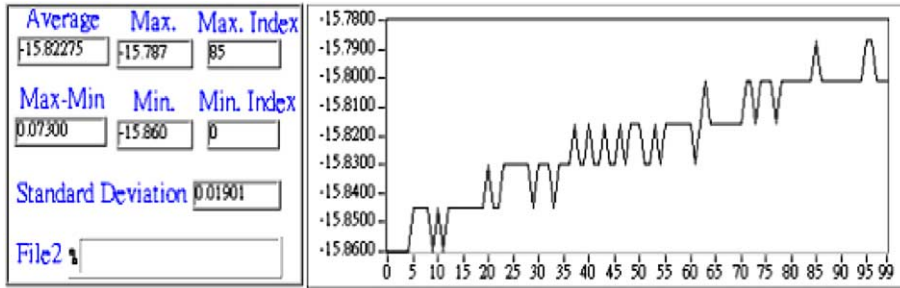
Fig. 13. The attenuation change through 100 cycles.

prove tuning range and reduce operation voltages using two actuator arrays. The experimental results confirmed the present to actuator arrays indeed reduce the operation voltages to 3.5 V. However, as shown in Fig. 6(a), the profile defection of the shutters make the faced-to-faced wedge-shaped shutters cannot isolate the incident light completely. Therefore the attenuation range can only achieved 28 dB.

In the following experimental results, only one thermal actuator array is activated to attenuate the light intensity. Fig. 10 shows the schematic measurement structure of VOA. An ASE light source via input fiber through shutter transmits to output fiber. The output fiber connects with power meter that can be converted to electric signal read by oscilloscope. The relationship of attenuation and displacement vs. voltage is shown in Fig. 11. When applied voltage is over 2 V, the thermal actuator moves over 5 μm that actuated the shutter to come into the optical path of fibers. At 4.5 V-applied voltages, the shutter covers the total optical path that obtains a maximum attenuation of 40 and 46 dB at 1550 and 1310 nm, respectively. The polarization dependent loss (PDL) is less 0.2 dB at attenuation less 20 dB. Unfortunately, as the attenuation is over 35 dB, the PDL increases to 1.5 dB. This drawback is produced by the diffraction effect at the poor shutter edge caused the higher PDL at higher attenuation range. The return loss at working situation is measured to be less than 45 dB. The return loss is higher than initial return loss due to light scattering from the roughness of the shutter. Redesign the shutter shape and controlling the fabrication technique can improve the outcome of PDL.

The dynamic response of the attenuator is shown in Fig. 12. A square signal is applied to the VOA resulting in attenuation between 1.23 and 40 dB. The rise time and fall time of thermal actuator is 3.44 and 2.2 ms, respectively. Note that, the phase shift of the test VOA is 1.2 ms. The response time of the thermal actuator array is compared with electrostatic comb drive fabricated by Marxer et al. which experienced 1 and 4.5 ms in rise time and fall time, respectively [6]. The more comb-fingers the larger displacement can be obtained and in return we increase the actuator mass and decrease response time. Furthermore, to demonstrate the reliability of the device, a 3 V square wave were used to drive the device about 100 cycles as shown is Fig. 13. The attenuation range changes from 15.787 to 15.86 dB and standard deviation is 0.019.

5. Conclusions

A compact VOA driving by thermal actuating principle with dual shutters for single mode fibers is developed in this paper. The structure is fabricated through the SOI-MEMS technology processes. The present process greatly simplifies the traditional surface micromachining technology and increases its corresponding reliability. Five different thermal actuator arrays have been designed and measured. They have similar characteristics that can cover full optical path (20 μm in the design) under 5 V. From experimental and simulation results, we concluded that the cross-shape tether can produce the best displacement efficiency.

References

[1] G.J. Veldhuis, F.N. Krommendijk, P.V. Lambeck, Opt. Commun. 168 (1999) 481.

[2] S.-S. Lee, Y.-S. Jin, Y.-S. Son, T.-K. Yoo, Ieee Photon. Technol. Lett. 11 (5) (1999).

[3] B.M. Andersen, S. Fairchild, N. Thorsten, V. Aksyuk, Mems variable optical attenuator for DWDM optical amplifiers, in: Optical Fiber Communication Conference 2000, vol. 2, 2000, p. 260.

[4] N.A. Riza, Fault-tolerant fiber-optical beam control modules, Patent No. 6,222,954, April 24, 2001.

[5] S. Sumriddetchkajorn, N.A. Riza, Opt. Commun. 205 (2002) 77.

[6] J.E. Ford, J.A. Walker, D.S. Greywall, K.W. Goossen, J. Lightwave Technol. 16 (9) (1998) 1663.

[7] MarxerbibfnmC., P. Griss, N.F. de Rooij, IEEE Photon. Technol. Lett. 11 (2) (1999) 233.

[8] S. Kim, S. Nam, Optical MEMS, in: IEEE/LEOS International Conference, August 2002, p. 65.

[9] C.-H. Kim, N. Park, Y.-K. Kim, MEMS reflective type variable optical attenuator using off-axis misalignment, in: Optical MEMS, IEEE/LEOS International Conference, August 2002, p. 55.

[10] T.-S. Lim, C.-H. Ji, C.-H. Oh, Y. Yee, J. Uk Bu, Electrostatic MEMS variable optical attenuator with folded micromirror, Optical MEMS, IEEE/LEOS International Conference, 2003, p. 143.

[11] R. Wood, V. Dhuler, Ed. Hill, A MEMS variable optical attenuator, in: Optical MEMS, IEEE/LEOS International Conference, August 2000, p. 121.

[12] V.R. Dhuuler, E.A. Hill, R. Mahadevan, M.D. Walters, R.L. Wood, MEMS variable optical attenuator, Patent No. US 6275320.

[13] C. Marxer, B. de Jong, N. de Rooij, Comparsion of MEMS variable optical attenuator designs, in: Optical MEMS, IEEE/LEOS International Conference, August 2002, p.189.

[14] R. Wayne, Fuchs, B. Keyworth, Micro-electro mechanical based optical attenuator, Pub. No.: US2002/076191.

[15] J.H. Comtois, V.M. Bright, Sens. Actuat. A 58 (1997) 19.

[16] M. Hoffmann, P. Kopka, E. Voges, Sens. Actuat. A 78 (1999) 28.

[17] A.A. Geisberger, N. Sarkar, M. Ellis, G.D. Skidmore, J. Microelectromech. Systems 12 (4) (2003).

[18] http://www.cxfiber.com.